Supplementary Information

Switchable Photoconductivity of Quantum Dot Films using Cross-Linking Ligands with Light-Sensitive Structures

G. Daniel Lilly,[a] Adam C. Whalley,[a] Sergio Grunder,[a] Cory Valente,[a] Matthew T. Frederick,[a] J. Fraser Stoddart,[a] and Emily A. Weiss[a]*

Department of Chemistry, Northwestern University 2145 Sheridan Road, Evanston, IL 60208-3113

*Corresponding author. Email: e-weiss@northwestern.edu

Materials and Methods

Materials. We used 90% trioctylphosphine oxide (TOPO), 90% trioctylphosphine (TOP), 90% hexadecylamine (HDA), selenium shot, 2.2-2.6% PEDOT:PSS in water, 99.99% eutectic gallium indium (EGaIn), and 95% dibenzenedithiol (BDT) as-purchased from Sigma Aldrich, cadmium stearate as purchased from MP Biomedicals, Inc., and 99.8% chloroform and 99.8% methanol as-purchased from VWR. Indium-tin-oxide (ITO)-coated glass (sheet resistance = 4-8 Ω) was provided by Delta Technologies Limited. Perfluoro-1,2-bis(2-iodo-5-methylthien-4-yl)cyclopentene was synthesized according to a literature procedure.[S1] Flash chromatography was performed using 300-400 mesh silica gel (Aldrich). ^{1}H NMR (500 MHz) and ^{13}C NMR (125 MHz) spectra were recorded on a Bruker AVANCE III 500 MHz spectrometer. All spectra were recorded at ambient temperature with the residual protons from the solvent as an internal reference. High-resolution mass spectra were measured on a Finnigan LCQ iontrap mass spectrometer (HR-ESI). All reactions were carried out under inert gas and photosensitive compounds were handled in the dark.

Synthesis of DAE Ligand and Precursors. *3-Bromo-tert-butylsulfanylbenzene (Figure S1B).* $AlCl_3$ (71 mg, 0.529 mmol) was added to a solution of 3-bromothiophenol (1.0 g, 5.29 mmol) and *tert*-butyl chloride (1.15 mL, 10.6 mmol) in MeCN (20 mL) in a flame-dried 50 mL round-bottom flask. The reaction mixture was heated under reflux for 48 h. On cooling, the mixture was added to H_2O and extracted with Et_2O (3 x 25 mL). The organic fractions were combined, dried ($MgSO_4$) and the solvent was removed under reduced pressure. The crude material was purified by silica gel chromatography eluting with hexanes to produce the desired product as a clear oil (986 mg, 76%). ^1H NMR (500 MHz, $CDCl_3$): $\delta = 7.70$ (t, $J = 1.8$ Hz, 1H), 7.50 (m, 1H), 7.46 (m, 1H), 7.21 (t, $J = 8.0$ Hz, 1H), 1.29 (s, 9H). ^{13}C NMR (125 MHz, $CDCl_3$): $\delta = 139.8$, 136.0, 135.0, 131.8, 129.8, 122.2, 46.50, 30.96.

3-(tert-Butylthio)phenylboronic acid (Figure S1C). 3-bromo-*tert*-butylsulfanylbenzene (500 mg, 2.04 mmol) was added to anhydrous THF (50 mL) in a flame-dried 100 mL round-bottom flask,and the reaction mixture was cooled to –78°C. *n*-BuLi (2.5 M in hexanes, 979 mL, 2.45 mmol) was added dropwise and the reaction mixture was left to stir at –78°C for 1 h. Triisopropyl borate (941 mL, 4.08 mmol) was added and the reaction mixture was left to warm to room temperature overnight. 1M HCl (25 mL) was added and the product was extracted with Et_2O (3 x 25 mL). The organic fractions were combined, dried ($MgSO_4$) and the solvent was removed under reduced pressure. The crude white solid was triturated with hexanes and employed in the next step without further purification.

Diarylethylene (DAE) (Figure S1D). In a 25 mL two-necked round-bottom flask equipped with a reflux condenser, THF (5 mL) and H_2O (2mL) were degassed by bubbling with nitrogen for 15 minutes. Perfluoro-1,2-bis(2-iodo-5-methylthien-4-yl)cyclopentene (140 mg, 0.226 mmol), 3-(*tert*-butylthio)phenylboronic acid (142 mg, 0.667 mmol), $Pd(PPh_3)_4$ (26 mg, 0.023

mmol), and K_2CO_3 (500 mg, 3.61 mmol) were added to this solution and the reaction mixture was stirred under reflux for 15 h. After cooling, the reaction was quenched with saturated $NH_4Cl_{(aq)}$ (25 mL) and extracted with CH_2Cl_2 (3 x 15 mL). The organic fractions were combined, dried ($MgSO_4$) and the solvent was removed under reduced pressure. The crude material was purified by silica gel chromatography eluting with hexanes to produce the desired product as a white solid (115 mg, 73 %). ^{1}H NMR ($CDCl_3$, 500 MHz): δ = 7.69 (t, *J* = 1.7 Hz, 4H), 7.53 (m, 2H), 7.46 (m, 2H), 7.35 (m, 3H), 7.28 (s, 2H), 1.98 (s, 6H), 1.31 (s, 18H). ^{13}C NMR ($CDCl_3$, 125 MHz): δ = 141.6, 141.4, 136.7, 134.3, 133.7, 133.6, 129.1, 125.9, 125.8, 122.7, 46.25, 31.02, 14.66. HRMS (ESI): *m/z* 697.1520, calcd for $C_{35}H_{35}F_6S_4$, *m/z* 697.1535 [$(M + H)^+$] found.

Compound **1** (110 mg, 0.158 mmol) and acetyl chloride (157 mL, 2.21 mmol) were dissolved in toluene (5 mL) in a flame-dried 25 mL round-bottom flask. BBr_3 (1.0 M in CH_2Cl_2, 347 mL, 0.347 mmol) was added dropwise to this solution and the reaction mixture was stirred at room temperature for 2 h. The reaction was quenched by pouring the mixture onto ice and the product was extracted with CH_2Cl_2 (3 x 15 mL). The organic fractions were combined, dried ($MgSO_4$) and the solvent was removed under reduced pressure. The crude material was purified by silica gel chromatography eluting with 50% CH_2Cl_2 in hexanes to produce the desired product as a white solid (46 mg, 43 %). ^{1}H NMR (CD_2Cl_2, 500 MHz): δ = 7.64 (m, 4H), 7.49 (m, 2H), 7.38 (m, 4H), 2.47 (s, 6H), 2.01 (s, 6H). ^{13}C NMR (CD_2Cl_2, 125 MHz): δ = 193.9, 142.8, 141.4, 134.7, 134.3, 131.8, 130.1, 129.6, 126.9, 126.2, 123.5, 30.54, 14.87. HRMS (ESI): *m/z* 669.0480, calcd for $C_{31}H_{23}F_6O_2S_4$, *m/z* 669.0474 [$(M + H)^+$] found.

Deprotection of S in DAE Ligand (The acetyl-protected DAE (17 mg, 0.025 mmol) was dissolved in CH_2Cl_2 (10 ml) and MeOH (40 ml). The mixture was degassed for 10 min. Acetyl chloride (1.0 ml) was then added dropwise, in order to form HCl *in situ*, over 30 min at room temperature. The reaction mixture was stirred for 60 min then evaporated and dried under high vacuum to give the free thiol DAE as a colorless solid (15 mg, 0.025 mmol). Since the free thiol is not stable it was deprotected prior to the physical investigations. Its structure was confirmed by HRMS (ESI): *m/z* 583.0123, calcd for $C_{27}H_{17}F_6S_4$, *m/z* 583.0122 $[(M - H)^-]$ found.

Synthesis and Purification of CdSe QDs. We synthesized CdSe QDs according to the method of Qu et al.,[S2] with minor modifications. We prepared a stock solution of 224 mmole TOP, 49.8 mmole cadmium stearate, and 46.8 mmole selenium, and injected 12 mL of the stock solution into a vigorously stirred mixture of 8.03 mmol HDA, 5.02 mmol TOPO at 320 °C under positive pressure N_2 atmosphere. The reaction mixture turned orange. We refluxed the mixture at 290 °C for 1 min, cooled it to 160 °C, and further quenched it by adding 15 mL of room-temperature $CHCl_3$ directly to the reaction flask. We purified the CdSe QDs from the solution by precipitating them three times from solvent/nonsolvent ($CHCl_3$/MeOH) suspension, redispersed them in $CHCl_3$,[S3] passed the resulting QD suspension in chloroform through a 0.5-μm filter, and stored the suspension in the dark in a closed vial in ambient environment for up to two months before depositing the films. The QDs for all samples were treated and stored identically. The CdSe QDs had an average diameter of 5.4 ± 1 nm as measured using TEM (Figure S2) and, after quenching with $CHCl_3$, a concentration of 10^{-5} M.[S4]

Ground State Absorption Spectroscopy. Ground state absorption spectroscopy measurements were performed with a Varian Cary 5000 spectrometer using a Cary 5000 solid sample holder. All measurements were performed on films deposited on ITO-coated glass slides.

Transmission Electron Microscopy. We mixed the CdSe QDs and ligands (DAE and BDT) in a ratio of 1000:1 ligand:QD, drop-cast the mixtures onto Ultrathin Carbon Film on Holey Carbon Support Films, 400 mesh copper TEM grids (Ted Pella, Inc.), and annealed at 120 ^{o}C for 30 min. The interparticle spacing of the DAE-CdSe QDs and BDT-QDs is estimated from 80 measurements over 10 transmission electron micrographs of each type of film with a JEOL 2100F FastTEM (Figure S5).

Atomic Force Microscopy. Atomic force spectroscopy (AFM) images were taken with a DI Scanning Probe Microscope in tapping mode using an *n*-type silicon App Nano SPM Probe (Figure S4). Samples consist of QD-Ligand Films on ITO/PEDOT:PSS; their preparation is discussed in the main text. The thickness of the film was obtained by scratching the film with an 18-gauge needle and scanned across the scratch. Three scratches were measured in two locations on each of three films (for each type of film), in order to calculate the average and standard deviation of the thickness. The thickness of the PEDOT:PSS layer (15.8 ± 0.4 nm) was subtracted from the total thickness to give the QD-ligand film thickness.

Formation of EGaIn Tip and QD Film Contact. The procedure for the formation of the EGaIn tip and subsequent contact with the QD film is described in detail elsewhere.[S5,S6] EGaIn is pulled into a 10 µL glass syringe and needle that is connected to an electrometer (Keithley 6430 sub-femtoamp remote source meter). A small droplet is extracted and contacted with an Au (or any metal)-coated Si substrate. The substrate is slowly lowered, drawing a tip with a diameter between 40 and 120 µm. The Au coated Si substrate is discarded and the QD film is placed under the tapered EGaIn tip. The QD film, which is on a stage controlled by a micro-manipulator, is slowly raised until contact is made with the EGaIn tip. The diameter of the tip is imaged with a digital camera and a calibrated computer screen. To ground the ITO, an Au-coated needle is connected to the electrometer and placed in contact with a corner of the QD film that has been cleaned to reveal the ITO substrate. Electrons flow from the ITO to the EGaIn under positive applied voltage, $V > 0$, and from EGaIn to ITO when $V < 0$.

Calculation of Expected Excited State Population, <*N*>. Consider a number of QDs, N_{QD}, within a circular area, A_s, illuminated by a number of photons, $N_{h\upsilon}$. If each QD has an absorption cross section σ_{QD}, then the fraction of quantum dots excited within the area of the spot, $\langle n\rangle$ is given by eq S1a. In eq S1, $J_{h\upsilon}$, is the photon density present within an infinitesimal

$$\langle n\rangle = \frac{N_{h\nu}N_{QD}\sigma_{QD}}{A_s N_{QD}} = J_{h\nu}\sigma_{QD} \tag{S1a}$$

$$J_{h\nu} = N_{h\nu}/A_s \tag{S1b}$$

slice of the sample. If we assume that the profile of the light is cylindrical, and that the sample absorbance is lower than $J_{h\upsilon}$, the absorbance can be considered constant throughout the sample, eq S1b. If the sample absorbance is significant, $J_{h\upsilon}$ will be thickness dependent, $J_{h\upsilon}(z)$, and attenuation of the light as is passes through the sample must be taken into account. Assuming Beer-Lambert behavior, $J_{h\upsilon}(z)$ can be integrated across the thickness of the sample, $\boldsymbol{\ell}$, eq 2. Integrating eq S2a using the relation S2b, the fraction of quantum dots excited within the

$$\langle n\rangle = \frac{1}{l}\int_0^l dzJ_0 10^{-\varepsilon zc}\sigma_{QD} = \frac{1}{l}\int_0^l dzJ_0 \exp[-\ln(10)\varepsilon_{QD}zc]\,\sigma_{QD} \tag{S2a}$$

$$\varepsilon = \frac{N_a\sigma}{\ln(10)} \tag{S2b}$$

illumination volume, $A_s\ell$, is given by eq S3, where N_a is Avagadro's number, ε is molar

$$\langle N\rangle = \frac{1000J_0}{N_a lc}(1-\exp[-\ln(10)\varepsilon lc]) \tag{S3}$$

absorptivity, and *c* is the concentration of quantum dots.

J-V Behavior of DAE Films (with no QDs). The junction with a DAE film with no QDs displays diode-like behavior: J at –1.0 V is, on average, a factor of 2 ± 1 times larger than J at +1.0 V (Figure S7). The DAE films show rectifying behavior for the same reason the QD-BDT films do: minimal dark current flows under positive bias, when EGaIn is depleted of electrons. The junction "turns on" under negative bias, when electrons flow from EGaIn through the DAE film and recombine with holes at the DAE/PEDOT:PSS interface. We can make three major observations about the data in Figure S7A: (i) there is no apparent photoconductivity of the films of DAE alone – that is, J measured under illumination is not greater than J measured in the dark for either green or UV illumination. (ii) The photocurrent does not "switch" with the wavelength of illumination in the absence of QDs—that is, J under UV illumination is not greater than J under green illumination. (iii) The current density of the DAE films degrades with time: J decreases by approximately ~81% at 1 V from the initial measurement period (DAE Closed, Illumination Source green [green circles], Figure S7A) to the final measurement period (DAE Open, Illumination Source UV [blue circles], Figure S7A). Figure S7B shows that this degradation is not just due to exposure to UV light: J also decreases (by, for example 62% at V = 1 V) during repeated J-V scans under constant illumination with green light for ~10 min.

The Effect of Pre-Illumination on J of the QD-DAE and QD-BDT Films. As we noted in the main text, one way to show that the switch in photoconductivity upon changing from green to UV illumination is not due to the differential photoresponse of the QDs, but rather to the conformational reorganization of the DAE ligand is to show that J for the QD-DAE films is sensitive to the time the QD-DAE films, where the initial state of the DAE is open (i.e., unconductive), were pre-illuminated with UV light; the longer the pre-illumination, the greater the population of DAE that are closed (i.e., conductive). Figure S8 shows a plot of J through an ITO/PEDOT:PSS/QD/EGaIn junction at an applied voltage of 1 V, where the QDs were cross-linked with DAE or BDT, as a function of time for two separate films. The films were first exposed to VIS (613-nm, power = 9.5 mW/cm^2) light for 30 minutes to prepare the ligands in an initially “open” (low-conductivity) geometry, and then with UV (366 nm) light for 40 min, where measurements of J were acquired every 2 minutes. The value of J through the QD-DAE films increased with longer illumination time as the DAE ligands progressively closed, while J for the QD-BDT films was insensitive to pre-illumination time. If the photoresponse of the films originated exclusively from the photoresponse of the QDs, J should not be sensitive to pre-illumination for the DAE films, and the insensitivity of the QD-BDT films to pre-illumination shows that the conductivity is not changing because of an illumination-induced charging phenomenon (such as photobrightening or photodarkening).

Stability of the QD-BDT Films. Figure S9 is a representative trace of J at 1V acquired over six illumination cycles over ~500 minutes; the illumination cycle is described in the caption. During this time, the average J through the QD-BDT films degraded by 22%, while J through a QD-DAE film that underwent the same illumination cycles did not degrade detectably.

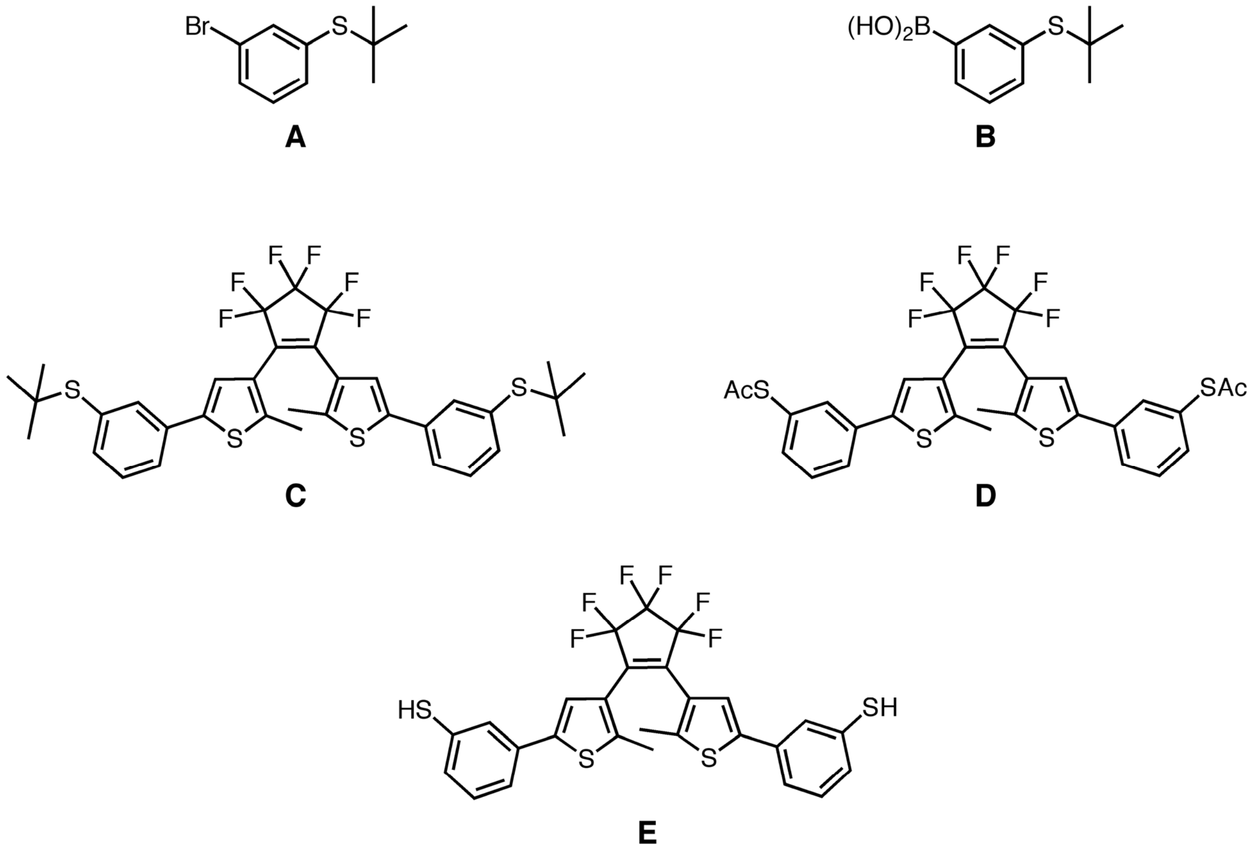

Figure S1. Structural formulas for (**A**) 3-bromo-*tert*-butylsulfanylbenzene, (**B**) 3-(*tert*-butylthio)phenylboronic acid, (**C**) *tert*-butyl protected DAE, (**D**) acetyl protected DAE (**E**) unprotected DAE.

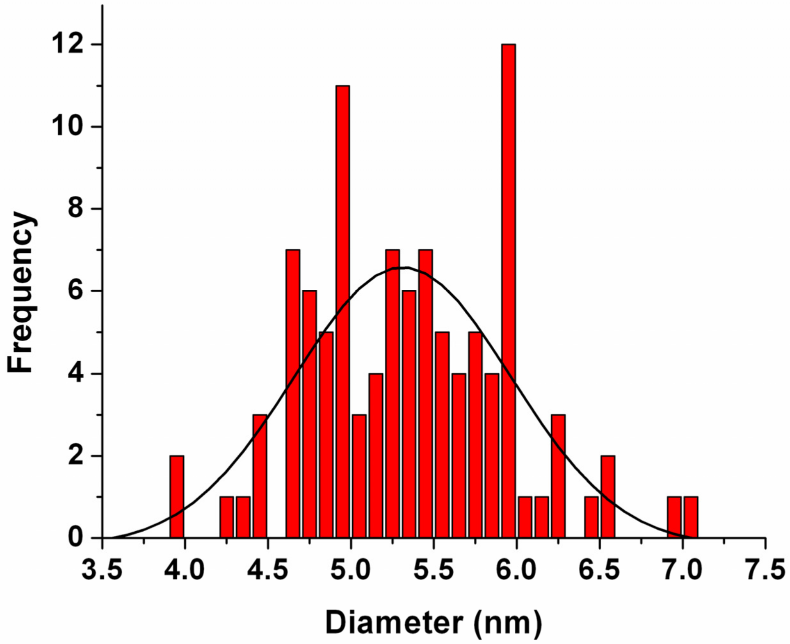

Figure S2. Representative histograms of the diameter (in nm) of CdSe QDs used in the films. The histogram is fit with a Gaussian function, and the mean and full-width-at-half-max of the Gaussian are used to determine the mean (5.4 nm) and standard deviation (1 nm) of the diameter of the CdSe QDs.

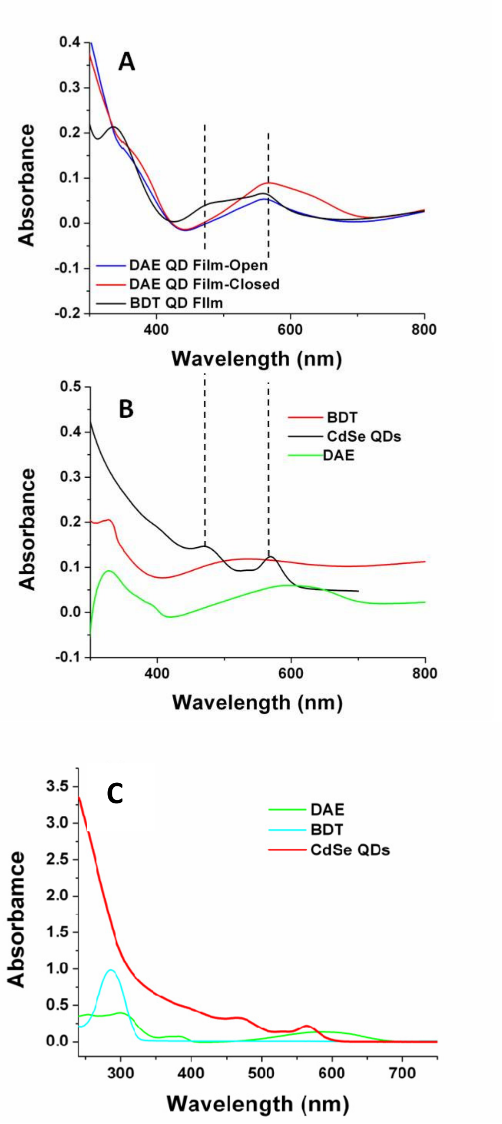

Figure S3. (**A**) Ground state absorption spectra of ITO-PEDOT:PSS-QD films cross-linked with DAE (DAE:QD = 1000:1) after exposure to 10 min of 366-nm (4.5 mW/cm^2) light (black) and 30 min of VIS light (red), and ITO-PEDOT:PSS-QD films cross-linked with BDT (DAE:QD = 1000:1). (**B**) Ground state absorption spectra of a film of CdSe QDs, a film of DAE, and a film of BDT spin-coated onto ITO. The dotted lines mark the wavelengths of the first distinct excitonic peaks of the QDs – where visible, these peaks are at the same wavelength in the QDonly film and in the QD-BDT/QD-DAE films. (**C**) For reference, the ground state absorption spectra of free DAE (~2×10^{-4}M), BDT (~4×10^{-3}M), and CdSe QDs (~1×10^{-5}M) in $CHCl_3$.

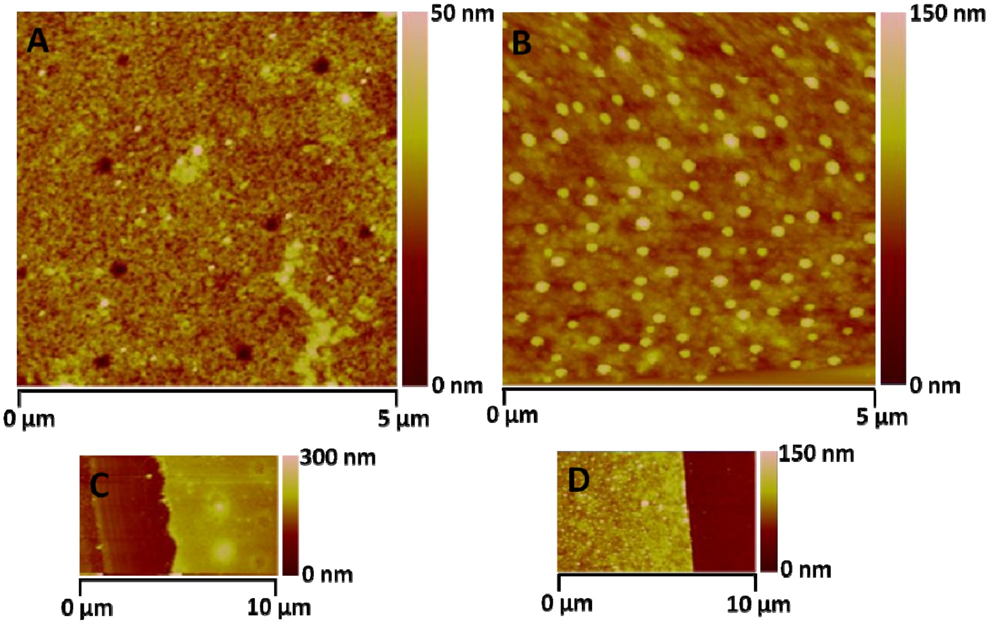

Figure S4. AFM images of QD films spun-cast onto ITO-glass, and cross-linked with DAE **(A, C)** and BDT **(B, D)**. Images **C** and **D** are of films that have been scratched with an 18-gauge needle in order to determine the thickness of the films. The QD-DAE film is 87.6 ± 13 nm thick with an RMS roughness of 4.7 nm over 25 μm^2 and the QD-BDT film is 38.3 ± 11.2 nm thick with an RMS roughness of 11.9 nm over 25 μm^2. The optical densities of the films were similar (BDT-QD: OD = 0.054, DAE-QD: OD = 0.066), so a similar number of QDs was deposited on each film; therefore, the difference in thicknesses is a result of the difference in interparticle distance, as dictated by the lengths of the cross-linking ligands. Three scratches were measured in two places on each film, and three films of each type were measured to calculate the averages and standard deviations.

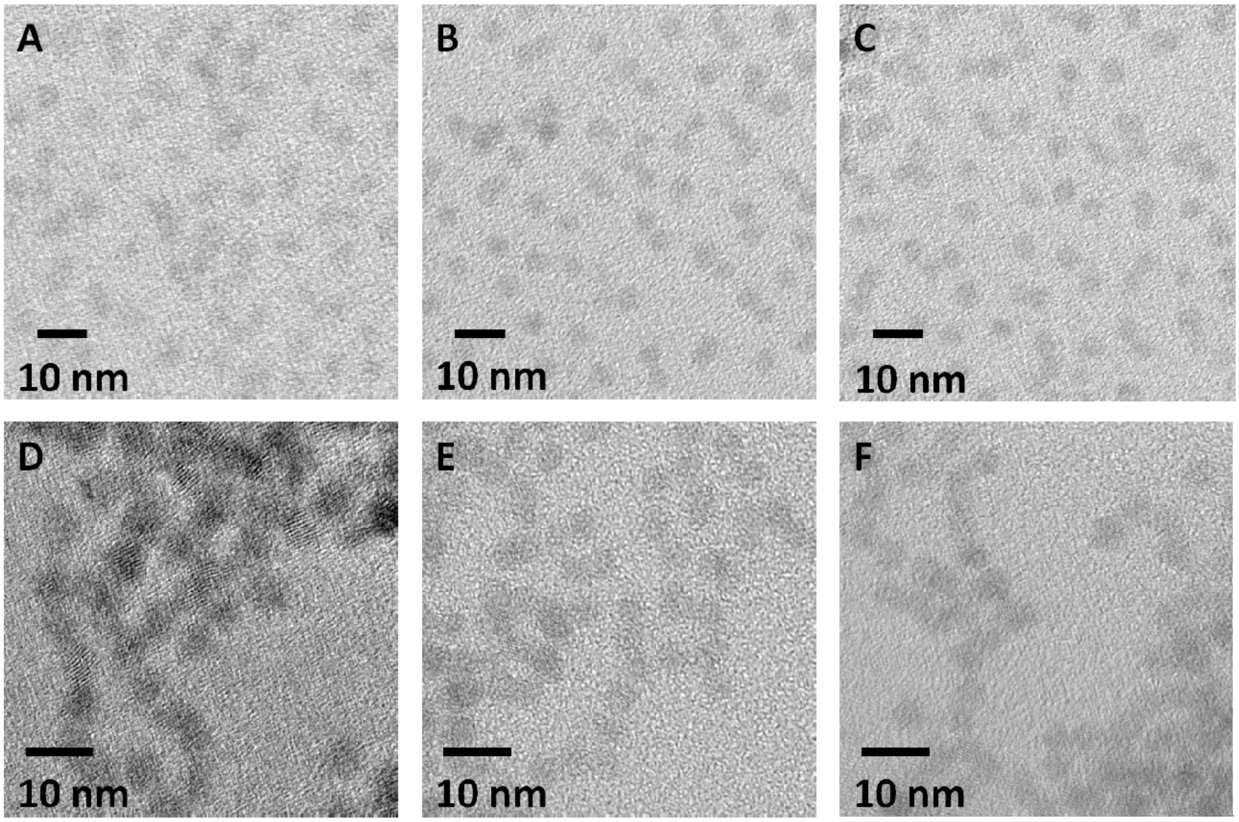

Figure S5. TEM images of the CdSe QDs treated with **A, B, C)** DAE and **D, E, F)** BDT. The samples are prepared by mixing the appropriate ligand with CdSe QDs in $CHCl_3$ at a molar ratio of 1000:1 (ligand:QD), stirring for 5 min, drop-casting the mixture onto a carbon on holey carbon TEM grid, and drying in a vacuum oven at 120 °C and 25” Hg for 30 min. The average inter-particle spacing (from 80 measurements over 10 images) is 18.1 ± 5 Å for the DAE-functionalized QDs, and 9.9 ± 4 Å for the BDT-functionalized QDs.

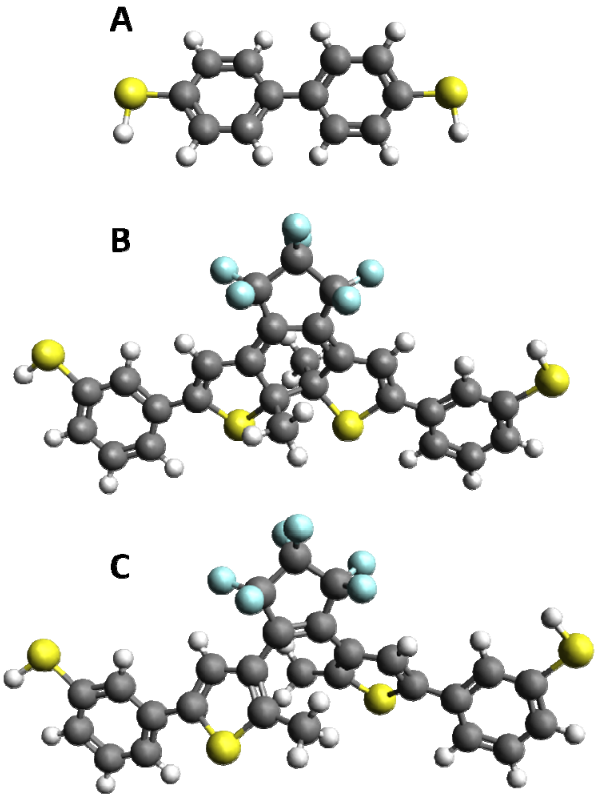

Figure S6. Optimized geometries for **(A)** BDT, **(B)** DAE closed, and **(C)** DAE open, calculated by DFT (B3LYP, 6-311G**). Hydrogen atoms are white, carbon atoms are dark gray, sulfur atoms are yellow, and fluorine atoms are light green. The cross-linking distance (S–S) was 10.7 Å for **A** and 16.7 Å for **B** measured using Avogadro: an open-source molecular builder and visualization tool (version 0.9.8. http://avogadro.openmolecules.net/).

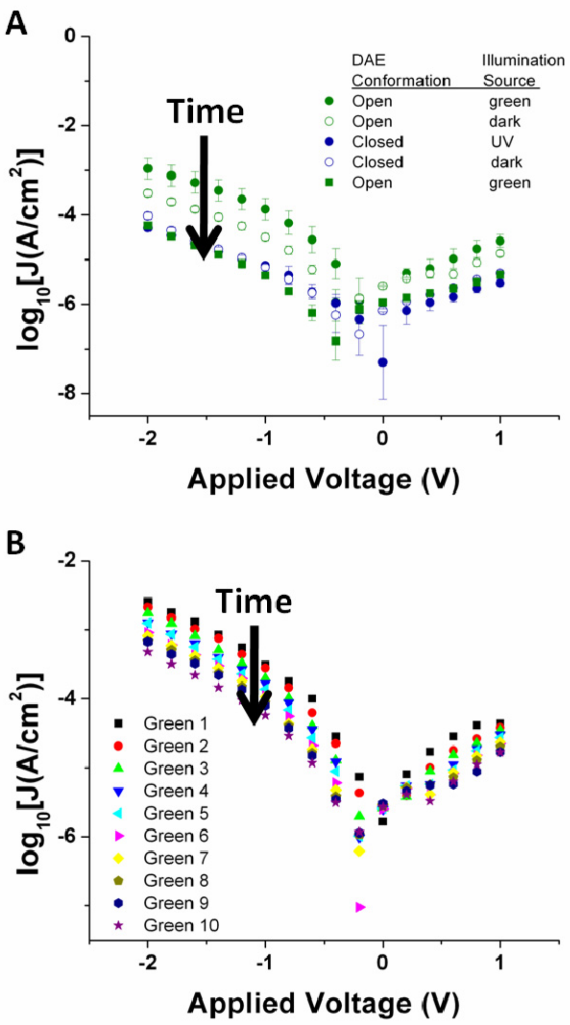

Figure S7. A) Plots of the average log of current density, J (A/cm^2), vs. applied voltage, V (V), for ITO/PEDOT:PSS/DAE/EGaIn junctions, where the DAE films contain no QDs, and illuminated according the scheme described in the legend; this illumination scheme is the same as that used for the QD-DAE films. The films were (i) illuminated with VIS (613-nm, power = 9.5 mW/cm^2) light for 30 min, (ii) excited with green (532-nm light, power = 1.1 mW/cm^2), while the current density was measured (green circles), (iii) placed in the dark, while current density was measured (open green circles), and (iv), illuminated with UV (366-nm light, power = 1.1 mW/cm^2) for 10 min, while the current density was measured (blue circles), and (v) placed in the dark while the current density measured (open blue circles). Each data point and error bars represent the log mean and standard deviation of 10 scans. **B)** Data for each of the ten individual scans under constant green illumination.

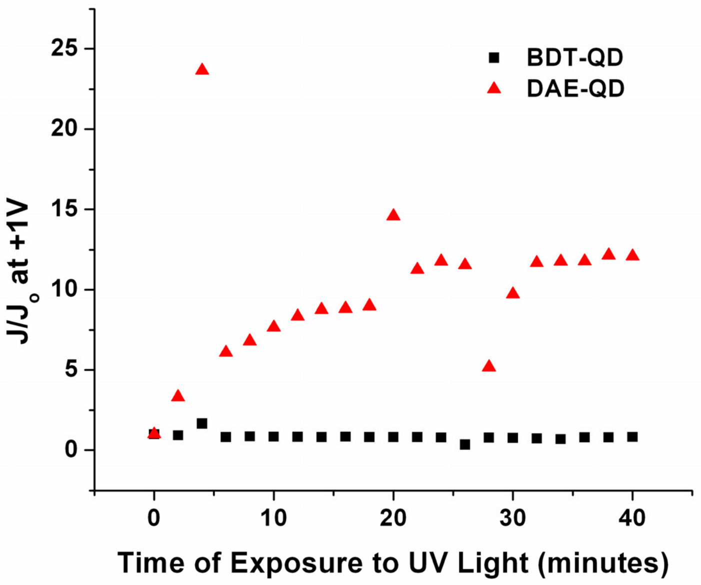

Figure S8. Current density (J) through an ITO/PEDOT:PSS/QD/EGaIn junction at an applied voltage of 1 V, where the QDs were cross-linked with DAE **(red)** or BDT **(black)**, as a function of time for two separate films. The films were first exposed to VIS (613-nm, power = 9.5 mW/cm^2) light for 30 minutes to prepare the ligands in an initially "open" (low-conductivity) geometry, and then with UV (366 nm) light for 40 min, where measurements of J were acquired every 2 minutes. The value of J through the QD-DAE films increased with longer illumination time as the DAE ligands progressively closed, while J for the QD-BDT films was insensitive to pre-illumination time.

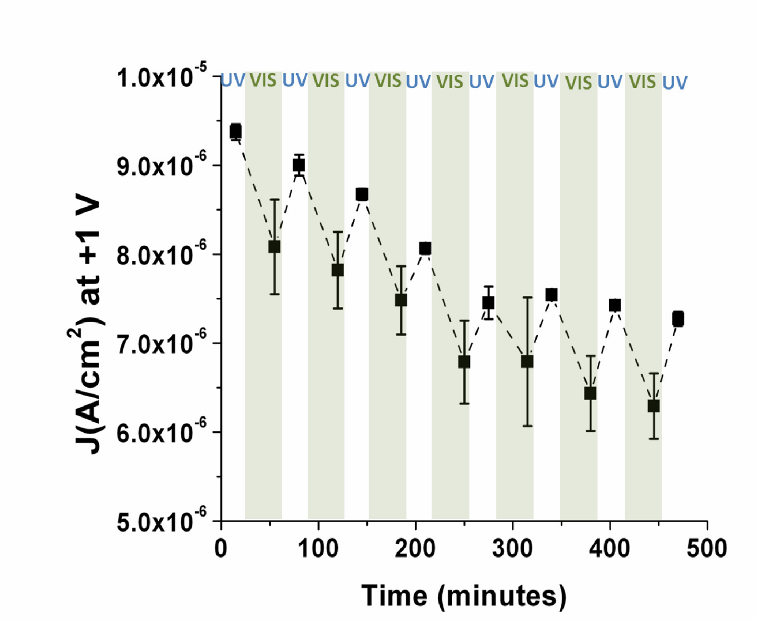

Figure S9. Current density (J) through an ITO/PEDOT:PSS/QD/EGaIn junction, where the QDs were cross-linked with BDT at an applied voltage of 1 V as a function of time over seven illumination cycles; the average on:off ratio was (1.1±0.4):1 and the current density (under both UV and green illumination) decayed by ~22% over six illumination cycles. Each cycle is as follows: (i) illumination with UV (366 nm) light for 10 min (shaded regions), (ii) illumination with UV (366 nm) light while the current density was measured at 1 V (10 min), (iii) illumination with VIS (613 nm light) for 15 min (white regions), and (iv) illumination with Green (532 nm light) while the current density was measured at 1 V (10 min). Each value of J is the linear average of 10 measurements on one junction (we did not acquire enough measurements to construct a histogram).

QD-DAE junctions – UV excitation

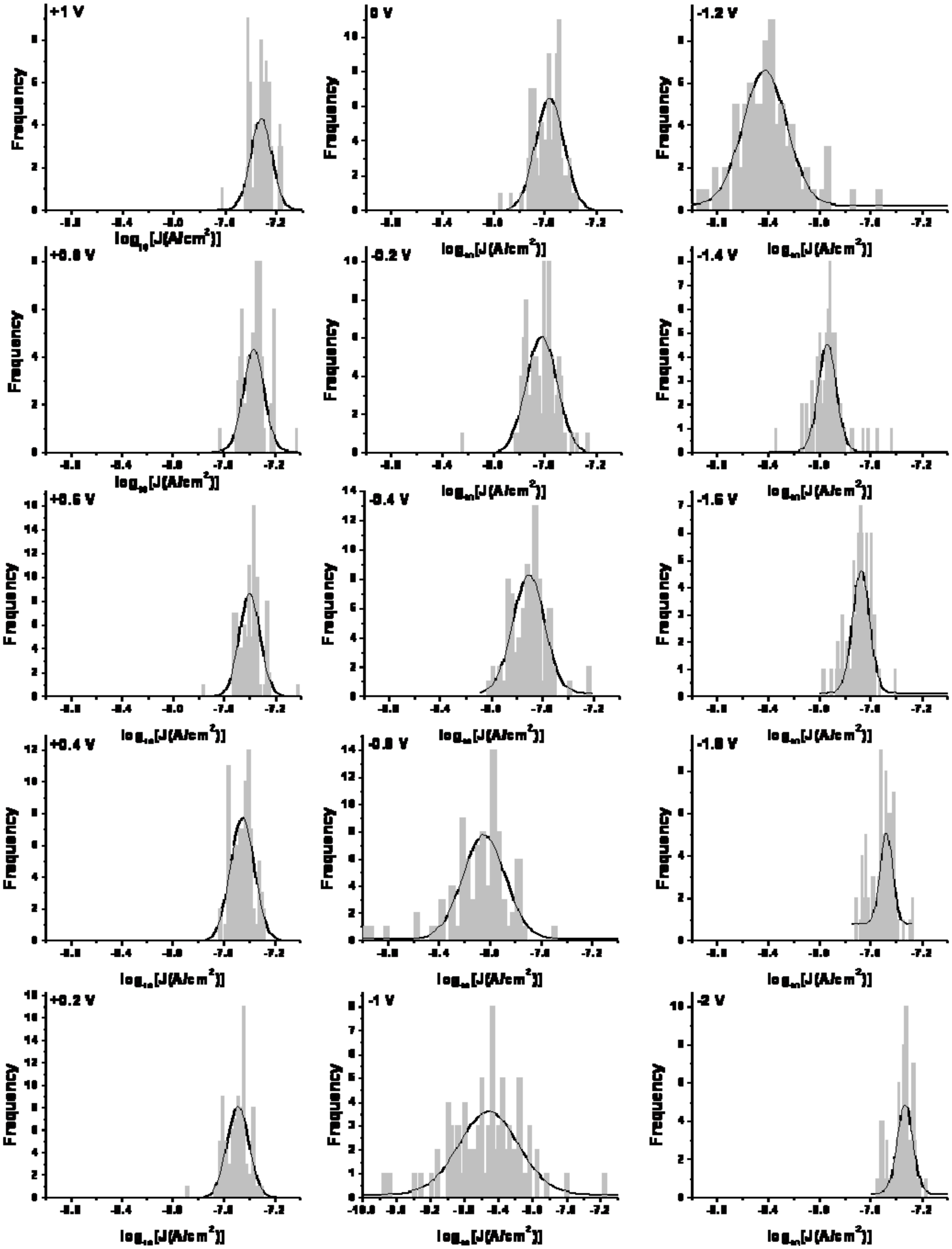

QD-DAE junctions – Green excitation

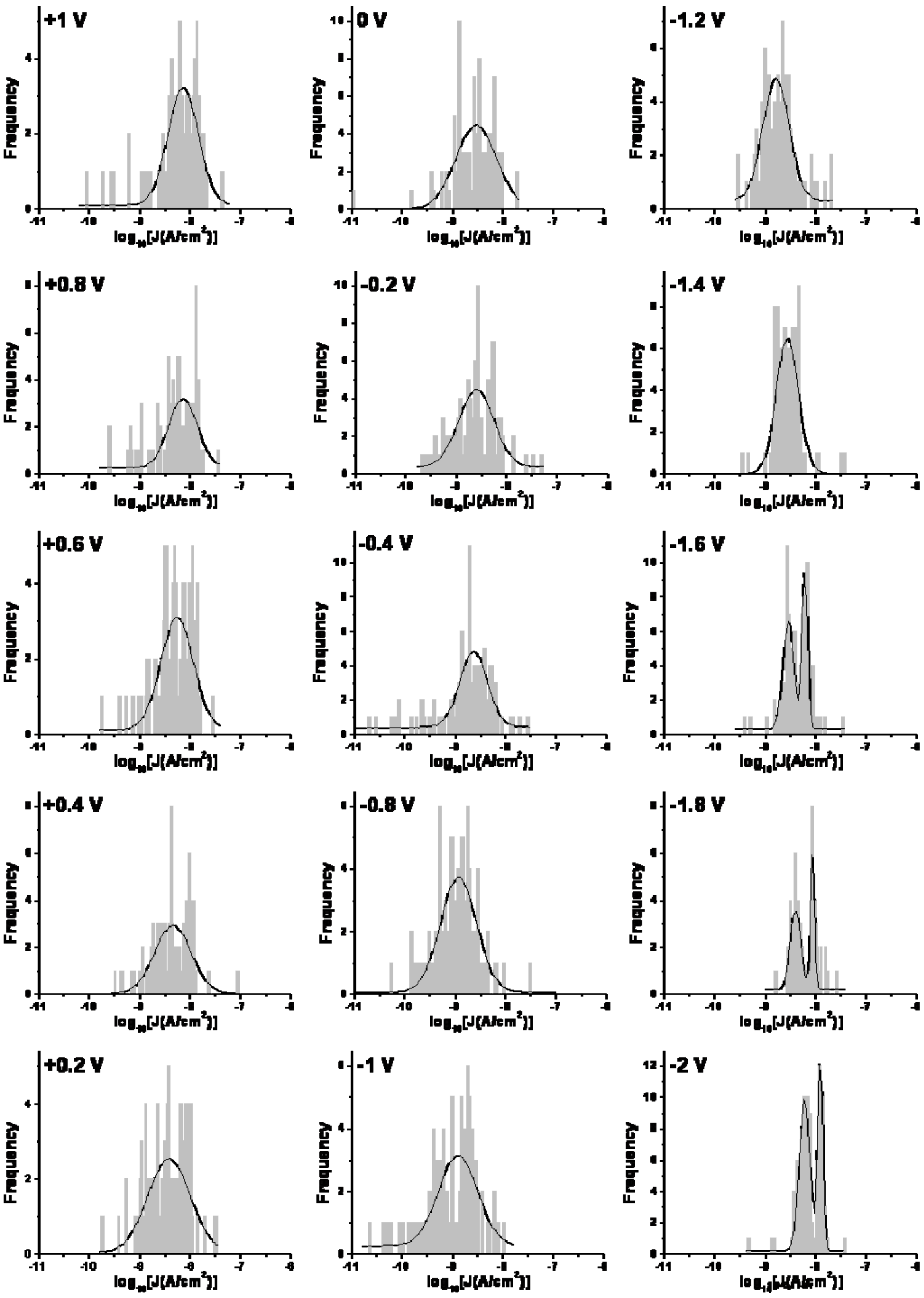

Figure S10. Representative histograms of $\log_{10}[J(A/cm^2)]$ for QD-DAE films at applied voltages from –2 V to +1 V for QD-DAE films illuminated with **A)** UV (366 nm) and **B)** Green (532 nm) light before and during the J-V scans. Each histogram is fit with a Gaussian function, and the peak and width of that Gaussian is used to determine the mean and error of each point in Figure 4A in the main text. There are no histograms for V = –0.6 V because these histograms are in the main text.

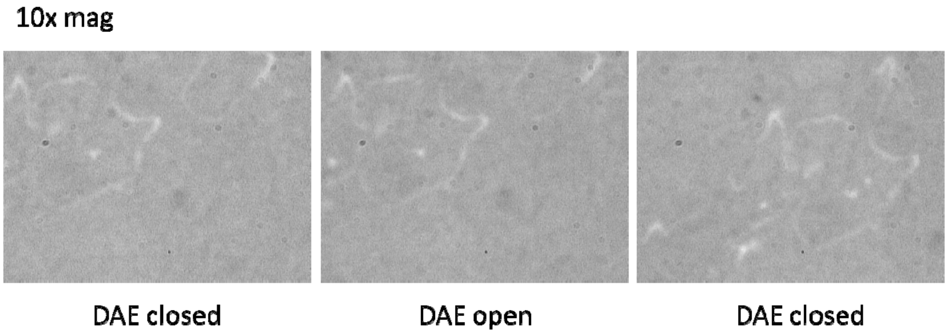

Figure S11. Microscope images at 10x magnification of the QD-DAE films as-deposited with DAE in the closed configuration (left), after illumination with VIS (613-nm) light for 30 minutes (middle), and after subsequent illumination with UV (366-nm) light for 20 minutes.

References

S1. S. Fraysse, C. Coudret and J. P. Launay, *Eur. J. Inorg. Chem.*, 2000, 1581.

S2. L. Qu and X. Peng, *J. Am. Chem. Soc.*, 2002, **124**, 2049.

S3. A. J. Morris-Cohen, M. D. Donakowski, K. E. Knowles and E. A. Weiss, *J. Phys. Chem. C*, 2010, **114**, 897.

S4. W. W. Yu, L. H. Qu, W. Z. Guo and X. G. Peng, *Chem. Mater.*, 2003, **15**, 2854.

S5. E. A. Weiss, R. C. Chiechi, S. M. Geyer, V. J. Porter, D. C. Bell, M. G. Bawendi and G. M. Whitesides, *J. Am. Chem. Soc.*, 2008, **130**, 74.

S6. E. A. Weiss, V. J. Porter, R. C. Chiechi, S. M. Geyer, D. C. Bell, M. G. Bawendi and G. M. Whitesides, *J. Am. Chem. Soc.*, 2008, **130**, 83.